



IL-6 mediates ER expansion during hyperpolarization of alternatively activated macrophages

Ehab A Ayoub^{1,2}, Karun Tandon^{1,2}, Manreet Padwal^{1,2}, Jewel Imani^{1,2}, Hemisha Patel^{1,2}, Anisha Dubey², Olivia Mekhael^{1,2}, Chandak Upagupta^{1,2}, Anmar Ayoub^{1,2}, Anna Dvorkin-Gheva², James Murphy^{1,2}, Philipp S Kolb^{1,2}, Sarka Lhotak³, Jeffrey G Dickhout³, Rick C Austin³, Martin R J Kolb¹, Carl D Richards²  & Kjetil Ask^{1,2} 

1 Department of Medicine, Firestone Institute for Respiratory Health, McMaster University and The Research Institute of St Joe's Hamilton, Hamilton, ON, Canada

2 Department of Pathology and Molecular Medicine, McMaster Immunology Research Centre, McMaster University, Hamilton, ON, Canada

3 Department of Medicine, Hamilton Centre for Kidney Research, McMaster University, Hamilton, ON, Canada

Keywords

ER expansion, IL-6, IRE1-XBP1, macrophage polarization, profibrotic macrophages

Correspondence

Kjetil Ask, Department of Medicine, McMaster University and The Research Institute of St. Joe's Hamilton, Firestone Institute for Respiratory Health, Luke Wing, Rm L314-5, 50 Charlton Ave East, Hamilton, ON, Canada L8N 4A6.
E-mail: askkj@mcmaster.ca

Received 21 November 2017;

Revised 24 June and 29 August 2018;

Accepted 3 October 2018

doi: 10.1111/imcb.12212

Immunology & Cell Biology 2019; **97**: 203–217

Abstract

Although recent evidence has shown that IL-6 is involved in enhanced alternative activation of macrophages toward a profibrotic phenotype, the mechanisms leading to their increased secretory capacity are not fully understood. Here, we investigated the effect of IL-6 on endoplasmic reticulum (ER) expansion and alternative activation of macrophages *in vitro*. An essential mediator in this ER expansion process is the IRE1 pathway, which possesses a kinase and endoribonuclease domain to cleave XBP1 into a spliced bioactive molecule. To investigate the IRE1-XBP1 expansion pathway, IL-4/IL-13 and IL-4/IL-13/IL-6-mediated alternative programming of murine bone marrow-derived and human THP1 macrophages were assessed by arginase activity in cell lysates, CD206 and arginase-1 expression by flow cytometry, and secreted CCL18 by ELISA, respectively. Ultrastructural intracellular morphology and ER biogenesis were examined by transmission electron microscopy and immunofluorescence. Transcription profiling of 128 genes were assessed by NanoString and Pharmacological inhibition of the IRE1-XBP1 arm was achieved using STF-083010 and was verified by RT-PCR. The addition of IL-6 to the conventional alternative programming cocktail IL-4/IL-13 resulted in increased ER and mitochondrial expansion, profibrotic profiles and unfolded protein response-mediated induction of molecular chaperones. IRE1-XBP1 inhibition substantially reduced the IL-6-mediated hyperpolarization and normalized the above effects. In conclusion, the addition of IL-6 enhances ER expansion and the profibrotic capacity of IL-4/IL-13-mediated activation of macrophages. Therapeutic strategies targeting IL-6 or the IRE1-XBP1 axis may be beneficial to prevent the profibrotic capacity of macrophages.

INTRODUCTION

Recently, the addition of the proinflammatory cytokine IL-6 was shown to enhance the M2-like macrophage phenotype, through the induction of IL-4-receptor expression enhancing the IL-4 response.¹ We have also demonstrated that IL-6 directly regulates macrophage profibrotic phenotype when combined with IL-4/IL-13 and substantiates lung fibrosis in the animal model.² More

recently, we also showed that of the gp130 cytokines IL-6, oncostatin M, and leukemia inhibitory factor, IL-6 was the only cytokine to directly mediate M2 macrophage programming *in vitro* and was associated with M2 macrophage accumulation in ectopic melanoma tumor growth *in vivo*.³ As these macrophages were hyperpolarized with the addition of IL-6, it provided a unique way to study mechanisms and organelles involved in the polarization process. Interestingly, the IRE1/XBP1 arm of

the unfolded protein response (UPR) is thought to play a role in the differentiation of various cell types, and this is believed to include monocyte to macrophage transition,⁴ eosinophil maturation,⁵ dendritic cell survival⁶ and B-cell to plasma cell differentiation.⁷ Plasma cell differentiation has been shown to be dependent on IRE1-XBP1 pathway and expansion of the endoplasmic reticulum (ER), required for antibody generation.⁷ The highly conserved endonuclease domain of IRE1 performs intracellular splicing of X-box binding protein 1 mRNA, critical in determining cell fate in response to ER stress in various cell types.⁸ In macrophages, spliced XBP1 has been shown to regulate the expression of many inflammatory cytokines such as IL-6, TNF α and others,^{9,10} while it was shown to be induced by IL-6 in B cells,⁷ suggesting varying biological function of spliced XBP1 and IL-6 in different cell types. Based on these observations, it would be logical to propose that the transformation and activation of specific cell types such as the wound-healing macrophage may involve the ER expansion program that is mediated by the IRE1-XBP1 pathway. The availability of IRE1 inhibitors would potentially prevent ER expansion and activation in these systems. Here, we hypothesized that the addition of IL-6 to macrophages exposed to the *in vitro* M2 activation cocktail IL-4 and IL-13 would lead to increased IRE1-XBP1 activation, leading to abundant ER expansion, associated with an increased secretory capacity that could be prevented by specific IRE1 inhibitors. Collectively, our data suggested that alternative macrophage polarization (achieved with IL-4/IL-13 stimulation) supplemented with the addition of IL-6 resulted in a much enhanced ER expansion associated with a dramatic increase in ER stress-associated gene expression. Furthermore, inhibition of the IRE1 pathway through treatment with STF-080310 prevented ER expansion and suppressed the M2 macrophage phenotype. This was observed *in vitro* through assessment of CD206 and arginase-1, two strong markers used to characterize M2-macrophage expression.^{2,11,12} Combined, the data presented suggest that therapeutic targeting of the IRE1 pathway or IL-6 signaling may prevent the profibrotic activity of M2-like macrophages *in vivo*.

RESULTS

IL-6-mediated alternative programming of macrophages leads to spliced XBP1 induction

To address the hypothesis that IL-6 addition to the standard alternative polarization cocktail IL-4/IL-13 mediates enhanced polarization and increased IRE1-XBP1 activation in a time-dependent manner, we developed a 96-well assay. In this experimental system,

bone marrow-derived macrophages (BMDMs) were seeded and exposed to different treatments and later assessed for arginase activity, arginase protein expression or spliced XBP1 gene expression in the cell lysates. The conventional cytokine cocktail IL-4/IL-13 or IL-4/IL-13/IL-6 were administered to BMDMs and assessed at 2, 4, 7, 15, 24 and 30 h. While the standard IL-4/IL-13 polarization cocktail alone resulted in a 2.9-fold increase in arginase activity at 30 h over naive macrophages (from 1.8 ± 0.36 mM urea per well at 2 h to 5.2 ± 4.85 at 30 h), the addition of IL-6 resulted in a 4.6-fold increase at 24 h and a 12-fold increase at 30 h (from 1.5 ± 0.11 mM urea per well at 2 h to 17.6 ± 4 at 30 h) (Figure 1a). Control macrophages or IL-6 stimulated macrophages demonstrated no increase in arginase activity at any of the indicated time points (data not shown). This increased arginase activity was associated with a strong arginase-1 protein expression at the 30-h mark, as demonstrated by western blotting (Figure 1b, please see Supplementary figure 1 for full western blot image). Of note, IL-6 alone did not modulate the expression of arginase-1 protein expression (Supplementary figure 1). Next, we assessed the activation of the IRE1-XBP1 axis by RT-PCR in BMDMs exposed to the IL-4/IL-13 or the IL-4/IL-13/IL-6-polarizing cocktails. Here, spliced XBP1 was modestly increased at 4 h (twofold) and maintained until later time-points (Figure 1c). The addition of IL-6 led to increased levels of spliced XBP1 that reached a 3.5-fold increase at 30 h (Figure 1c). These data suggest that IL-6 addition leads to increased polarization and activation of the IRE1-XBP1 pathway. As IRE1-XBP1 has been shown to be required in the induction of ER membrane biogenesis programs in various cell types activated toward a secretory phenotype,^{5,13,14} we next investigated if the addition of IL-6 influenced ER expansion in alternatively activated macrophages.

IL-6 enhances ER expansion in alternatively activated macrophages

BMDMs were polarized as described above and examined by transmission electron microscopy. As evaluated under the electron microscope, BMDMs treated with IL-4/IL-13 had a prominent stacked ER (Figure 2a and Supplementary figure 2), suggesting enhanced membrane biogenesis, as well as accumulation of sizable mitochondria, suggesting enhanced metabolic activity. In addition, we used immunofluorescence labeling of KDEL to quantify ER expansion or size. KDEL is a well-regarded peptide sequence marker that allows proteins to be retained in the ER indicative of ER expansion.^{15,16} Consistent with the transmission electron microscopy data,

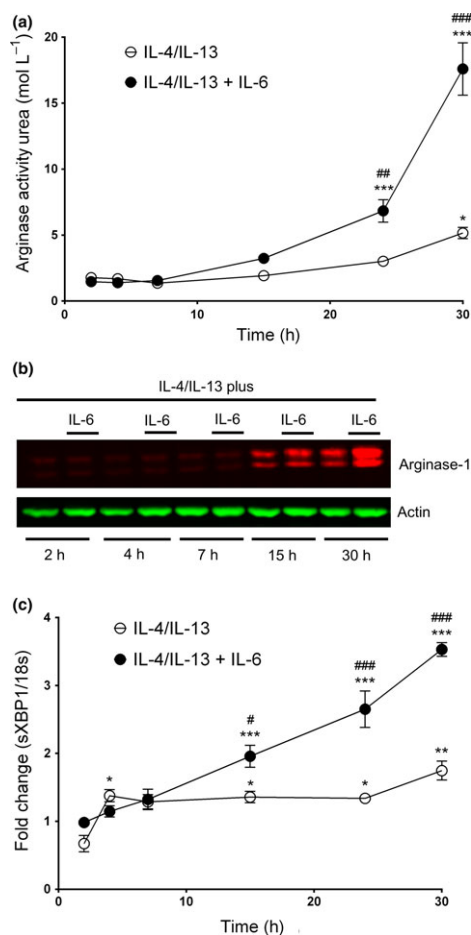


Figure 1. IL-6 addition promotes macrophage M2 polarization and spliced XBP1 induction. BMDMs were exposed to the M2 polarization cocktail IL-4/IL-13 alone (open circles) and with the addition of IL-6 (closed circles). Cell lysates were assessed for **(a)** arginase activity at 2, 4, 7, 15, 24 and 30 h, values were expressed as mmol urea per well and **(b)** arginase-1 protein. **(c)** In a separate experiment, mRNA was extracted from cell lysates and assessed for the appearance of spliced XBP1 at 2, 4, 7, 15, 24 and 30 h. A one-way ANOVA was used to assess the effect of each treatment and to identify at which time point each treatment was different from their respective controls (2 h) and indicated with *. Data are presented as mean \pm s.e.m., each time point was assessed in quadruplicates. *, # indicates $P < 0.05$; **, ## indicates $P < 0.01$; ***, ### indicates $P < 0.001$; where * represents a difference between any sample relative to the control sample within the same group; # represents a difference between the two different groups at the indicated time point.

there was an increase in KDEL expression in IL-4/IL-13/IL-6 stimulated BMDMs (Figure 2b, d). The potent IRE1 inhibitor STF-083010, known to inhibit IRE1 endonuclease activity and mRNA splicing of XBP1 was added to the conventional IL-4/IL-13 polarization cocktail and to IL-4/IL-13/IL-6-mediated hyperpolarizing cocktail. KDEL expression was abrogated with the addition of the sXBP1

inhibitor, STF-083010 (Figure 2b, d). Of note, Tunicamycin treatment alone, which is expected to enhance ER membrane biogenesis because of the accumulation of unfolded proteins, also induced an increase in KDEL expression. In the same fashion, we used TOMM20, which is a major mitochondrial protein receptor that is widely used as a biomarker to identify and quantitate mitochondrial density and oxidative phosphorylation.¹⁷⁻¹⁹ As expected, TOMM20 was highly augmented, reflecting an increase in both mitochondrial size and numbers (Figure 2c, d). These findings combined with transmission electron microscopy evidence demonstrate that both ER and mitochondrial membrane expansion occur in macrophages stimulated with IL-4/IL-13/IL-6 and can be modulated pharmacologically with the IRE1 inhibitor, STF-083010. Thus, the data presented in Figures 1 and 2 suggest that the stepwise increase in macrophage alternative activation, as mediated by IL-6, is associated with IRE1-XBP1 activation and increased ER expansion. Based on these observations, we then examined if ER expansion is associated with the induction of key UPR-related markers.

IL-6 enhances the expression of select UPR markers

To address the hypothesis that ER expansion in IL-4/IL-13/IL-6-stimulated macrophages is associated with enhanced UPR activation, murine BMDMs were exposed to IL-4/IL-13, IL-4/IL-13/IL-6 alone or with the addition of STF-083010. UPR activation was assessed by immunofluorescence staining of the general UPR markers: cleaved ATF6, p-PERK and ATF4. Quantification of the percent positive area per cell demonstrated that ATF6 was highly induced in IL-4/IL-13/IL-6-stimulated cells; which has been observed to be associated with ER expansion. A partial but not complete reduction in ATF6 was seen with STF-083010 treatment, suggesting that sXBP1 inhibition could indirectly affect ATF6 cleavage or activation (Figure 3a, d). Although we did not observe a significant alteration of p-PERK in all conditions compared to control, we saw a marked downregulation of the downstream target, ATF4, which was partially restored with STF-083010 treatment (Figure 3b-d).

IRE1-XBP1 inhibition prevents IL-6-mediated alternative activation of macrophages

Based on the observations in Figures 1-3, we examined whether pharmacological inhibition of the IRE1-XBP1 pathway affected IL-6-mediated polarization of alternatively activated macrophages. Arginase activity and spliced XBP1 mRNA were measured in cell lysates after incubation with STF-083010. Figure 4a shows IL-4/IL-13-mediated polarization of murine BMDMs for 30 h led to

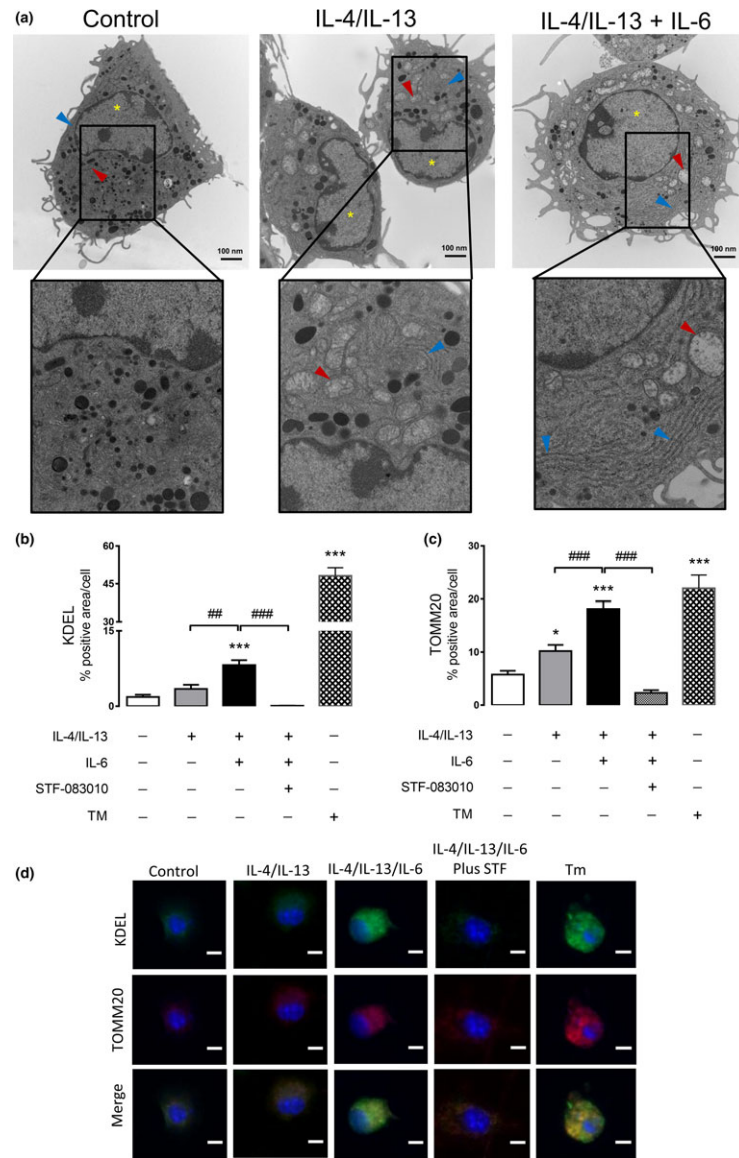


Figure 2. IL-6 addition to IL-4/IL-13 promotes ER expansion and mitochondrial membrane biogenesis. After exposing BMDMs to the M2 polarization cocktail IL-4/IL-13 alone, and with the addition of IL-6, for 30 h, transmission electron microscopy was performed. In a separate experiment, the same conditions were repeated with the addition of IL-4/IL-13/IL-6+STF-083010 and tunicamycin, as a positive control. Here, cells were subjected to immunofluorescence staining and quantification of KDEL and TOMM20. **(a)** Transmission electron microscopy images showing BMDMs polarized with IL-4/IL-13 and IL-14/IL-13+IL-6. The red and blue arrowheads show mitochondria and endoplasmic reticulum, respectively; the yellow asterisks indicate the location of the nucleus. Scale bar = 100 nm. **(b, c)** Immunofluorescence quantification of KDEL (green) and TOMM20 (red) and **(d)** representative images showing the staining. Scale bar = 5 μm. Bar graphs represent mean ± s.e.m. from at least 50 cells per condition. * indicates $P < 0.05$; ## indicates $P < 0.01$; ***; ### indicates $P < 0.001$; where * represents a difference between any sample relative to the control unexposed group; # represents a difference between the indicated groups.

an increase in arginase activity, that was reduced by the addition of STF-083010 at a non-toxic concentration of 60 μM (Supplementary figure 3). The prevention of arginase activity was associated with a decrease in spliced XBP1 mRNA (Figure 4b), suggesting that the IRE1-XBP1 axis is involved in alternative programming of macrophages. As a positive control, Tunicamycin was used

to stimulate sXBP1 induction, which was attenuated with the addition of STF-083010 (Supplementary figure 4). However, induction of ER stress by tunicamycin treatment alone did not induce macrophage M2 polarity, as assessed by arginase activity (Supplementary figure 5). As shown above, the addition of IL-6 to the standard IL-4/IL-13 polarization cocktail resulted in a 5.4-fold increase in

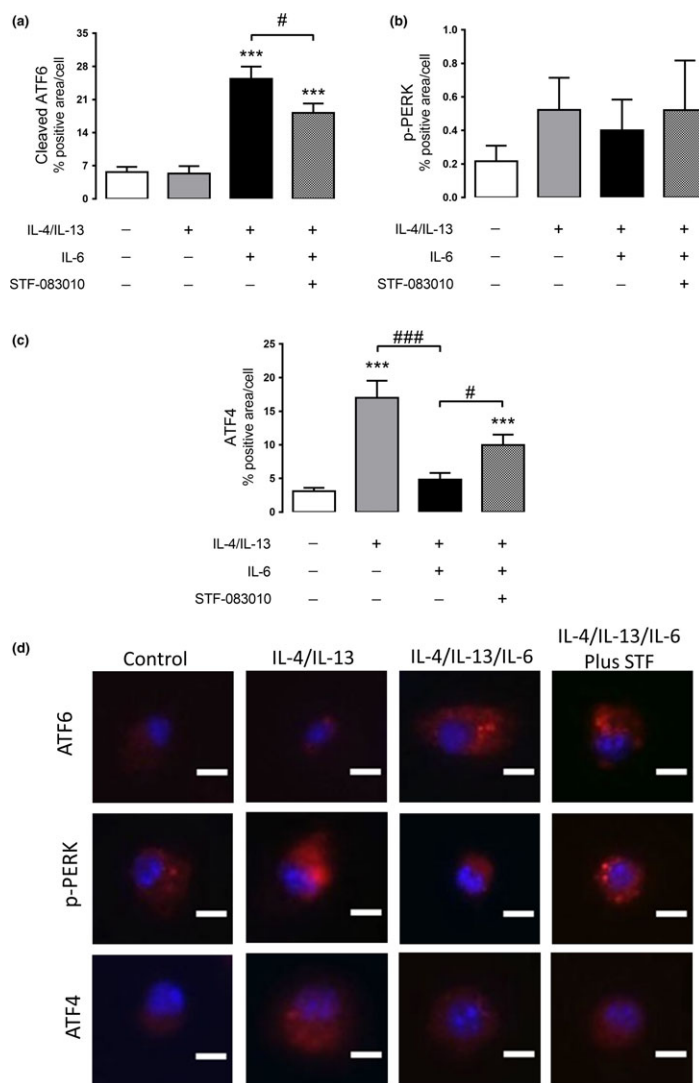


Figure 3. IL-6 addition to IL-4/IL-13 induces the expression of key UPR-related markers. BMDMs were cultured for 30 h with IL-4/IL-13 or IL-4/IL-13+IL-6, alone or in combination with STF-083010 (60 μ M). Cells were then subjected for immunofluorescence staining of ATF6, p-PERK and ATF4. Immunofluorescence quantification was performed to show the percent positive area per cell for **(a)** ATF6 **(b)** p-PERK and **(c)** ATF4. **(d)** Representative images are shown from the three assessed markers. Scale bar = 5 μ m. Bar graphs represent mean \pm s.e.m. from at least 50 cells per condition. # indicates $P < 0.05$; ***; ### indicates $P < 0.001$; where * represents a difference between any sample relative to the control unexposed group; # represents a difference between the indicated groups.

arginase activity (from 2.0 ± 0.88 mM Urea per well to 10.7 ± 2.44 , expressed as mean \pm s.e.m.). The addition of IRE1-XBP1 inhibitor led to a 55% decrease in arginase activity as well as a robust inhibition of spliced XBP1 at 60 μ M STF-083010, confirming the likely involvement of the IRE1-XBP1 pathway in IL-6-mediated hyperpolarization of macrophages. Furthermore, we examined phagocytic capacity of macrophages by assessing the uptake of fluorescently labeled nanoparticles. We observed that STF-083010 (60 μ M) addition to IL-4/IL-13/IL-6 significantly reduced the phagocytic ability of these cells (Supplementary figure 6).

To further consolidate the finding that XBP1 inhibition prevents IL-4/IL-13-mediated alternative programming of macrophages and IL-6-mediated hyperpolarization, we performed flow cytometric analysis of the well-established alternative macrophage flow markers arginase-1 and CD206 to the different cocktails and treatments shown above. A figure exemplifying the gating strategy of the target population is presented in the online supplement (Supplementary figure 7). Arginase-1/CD206 levels were increased from less than 20% to 52.8% after IL-4/IL-13 exposure and further increased to 73.6% when IL-6 was added (Figure 4c), which is consistent with recently

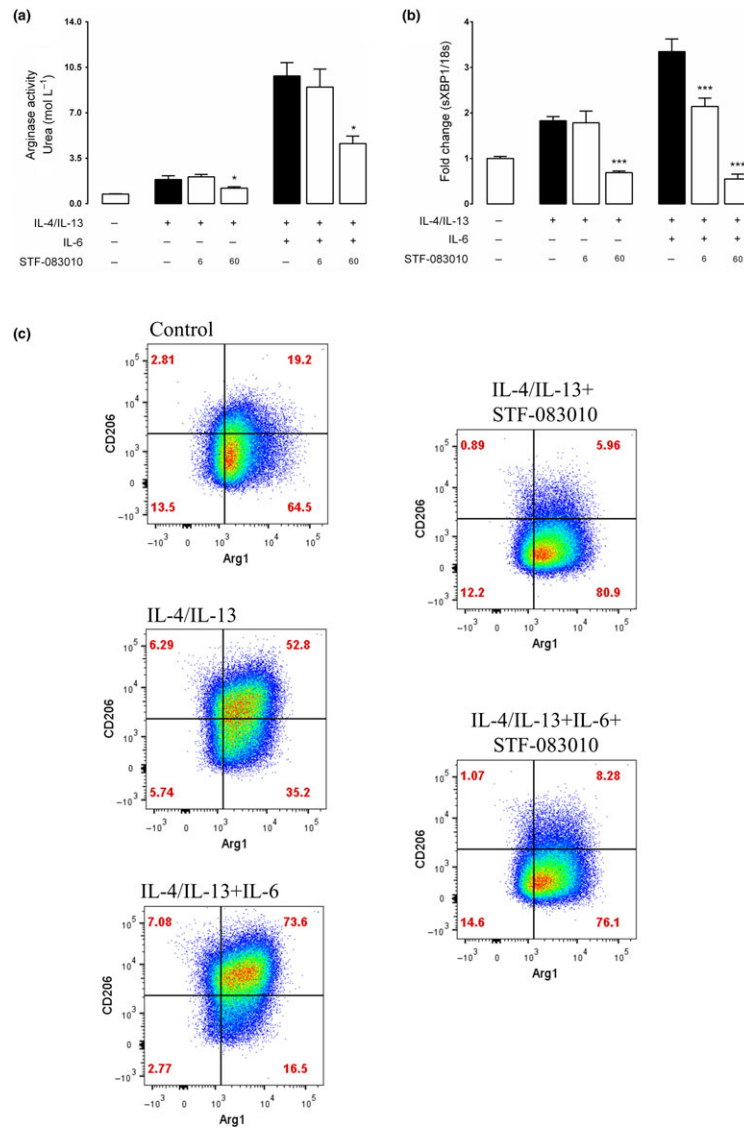


Figure 4. Inhibition of IRE1-XBP1 splicing reduces macrophage alternative activation following their hyper-polarization with IL-6. BMDMs were cultured for 30 h with IL-4/IL-13 or IL-4/IL-13+IL-6, alone or in combination with STF-083010 (6 and 60 μ M). **(a)** Arginase activity, which is reflective of the M2 macrophage phenotype, was assessed in cell lysates, and later accompanied with **(b)** RT-PCR of sXBP1. **(c)** Representative flow cytometric plots of selected samples showing the frequency of arginase-1/CD206 positive cells during macrophage polarization with/without STF-083010. Bars represent mean \pm s.e.m. from four replicates per group and graph is representative of two independent experiments. Two black-filled columns were included, in which one serves as reference control for IL-4/IL-13 stimulated groups and other for IL-3/IL-13/IL-6 stimulated groups. * indicates $P < 0.05$; *** indicates $P < 0.001$; where * represents a difference between white-filled columns and the reference control.

published observations.² The addition of the IRE1-XBP1 inhibitor STF-083010 prevented both IL-4/IL-13 and IL-4/IL-13/IL-6-mediated polarizations with less than 10% arginase-1/CD206 positive macrophages detected (Figure 4c). These findings collectively suggest that the induction of ER stress alone in macrophages is insufficient to drive M2 macrophage programming and that XBP1 blockade markedly inhibit both conventional

IL-4/IL-13-mediated alternative programming as well as IL-6-mediated hyperpolarization of macrophages. To better understand the functional effect of IL-6-mediated hyperpolarization of alternatively activated macrophages and the effect of IRE1 inhibition, we next examined more broadly the gene expression pattern as well as the cytokine production of the different polarization cocktails described above.

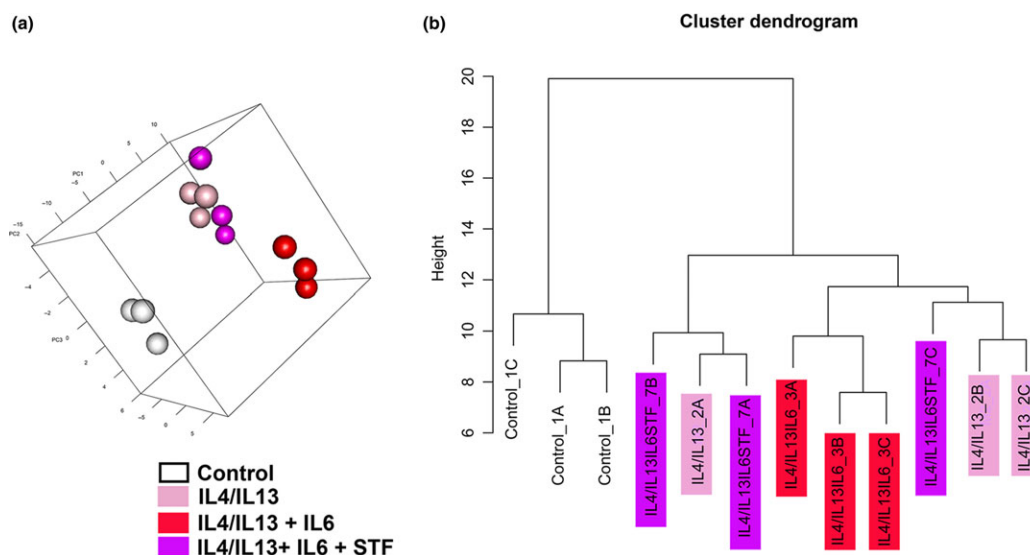


Figure 5. Principal component analysis plot and hierarchical clustering of the samples showing the ability of STF-083010 to normalize the transcriptional signature of hyper IL-4/IL-13/IL-6 stimulated macrophages to IL-4/IL-13 stimulated macrophages. IL-6 BMDMs were cultured for 30 h with IL-4/IL-13, IL-4/IL-13+IL-6 and IL-4/IL-13+IL-6+STF-083010 and subsequently subjected for RNA isolation and NanoString gene expression. **(a)** Principal component analysis (PCA) plot, presenting the four groups. **(b)** Dendrogram, obtained from hierarchical clustering of the same samples (using euclidean distance and average linkage).

IRE1-XBP1 inhibition reduces the profibrotic- and chaperone-expressing capacity of IL-6-mediated alternative activation

Murine BMDMs were exposed to IL-4/IL-13 and IL-4/IL-13/IL-6 and STF-083010 for 30 h as described above. RNA was extracted from the cell lysates and subjected to NanoString(R) assessment of 128 inflammatory, UPR and fibrotic related genes (see Supplementary table 1 for information about all genes investigated). Principal component analysis and hierarchical clustering of the samples demonstrated a unique transcriptional signature of IL-4/IL-13/IL-6 stimulated macrophages compared to other treatment conditions (Figure 5a). Upon examination of the plots of the assessed samples as evidenced by the cluster dendrogram, the data show that samples treated with STF-083010 plus the IL-4/IL-13/IL-6 cocktail cluster in a similar fashion to IL-4/IL-13 exposed samples, suggesting that STF-083010 might have normalized the transcriptional signature of IL-4/IL-13/IL-6-exposed macrophages to IL-4/IL-13-exposed macrophages (Figure 5b). To quantitatively and qualitatively understand the meaning of the assessed transcriptional signature, differentially regulated genes were presented as a table showing pair-wise comparisons of interest (Figure 6a) demonstrating the number of upregulated and downregulated genes within the specified groups. Functional networks were then established based on the assessed gene signature, and processes were illustrated by

ellipses, with multiples genes of interest comprising eight modules (Figure 6b, c). For an enlarged functional network detailing the different pathways, please see Supplementary figure 8. As we have recently shown that exogenous adenoviral administration of IL-6 potentiates the alternative activation of macrophages and the enhanced response to bleomycin-induced lung fibrosis *in vivo* and that the *in vitro* addition of STF-083010 to IL-4/IL-13/IL-6 abolished the expression of *Fnl1*, *Mcp1* and *Timp1* to almost control levels,² we next examined if the enhanced profibrotic/alternatively activated phenotype was associated with an increase in the expression of the ER-resident molecular chaperones; *Xbp1*, *Grp78* and *Calreticulin* (Figure 6d). As with our earlier observation with *Fnl1*, *Mcp1* and *Timp1*, the addition of STF-083010 prevented IL-4/IL-13/IL-6-mediated increase in the expression of *Xbp1*, *Grp78* and *Calreticulin*. Overall, these findings suggest that STF-083010 reduces the hyperprofibrotic M2-like phenotype as well as the ER-chaperone expressing capacity of macrophages elicited by IL-4/IL-13 and IL-6.

STF-083010 prevents IL-4/IL-13/IL-6-mediated CCL18 secretion and hyperpolarization of human macrophages

To examine whether our findings in murine BMDMs could be replicated in a human setting, we investigated the effect of IL-4/IL-13+IL-6 polarization in the well-characterized PMA-activated THP-1 macrophage cell line. During

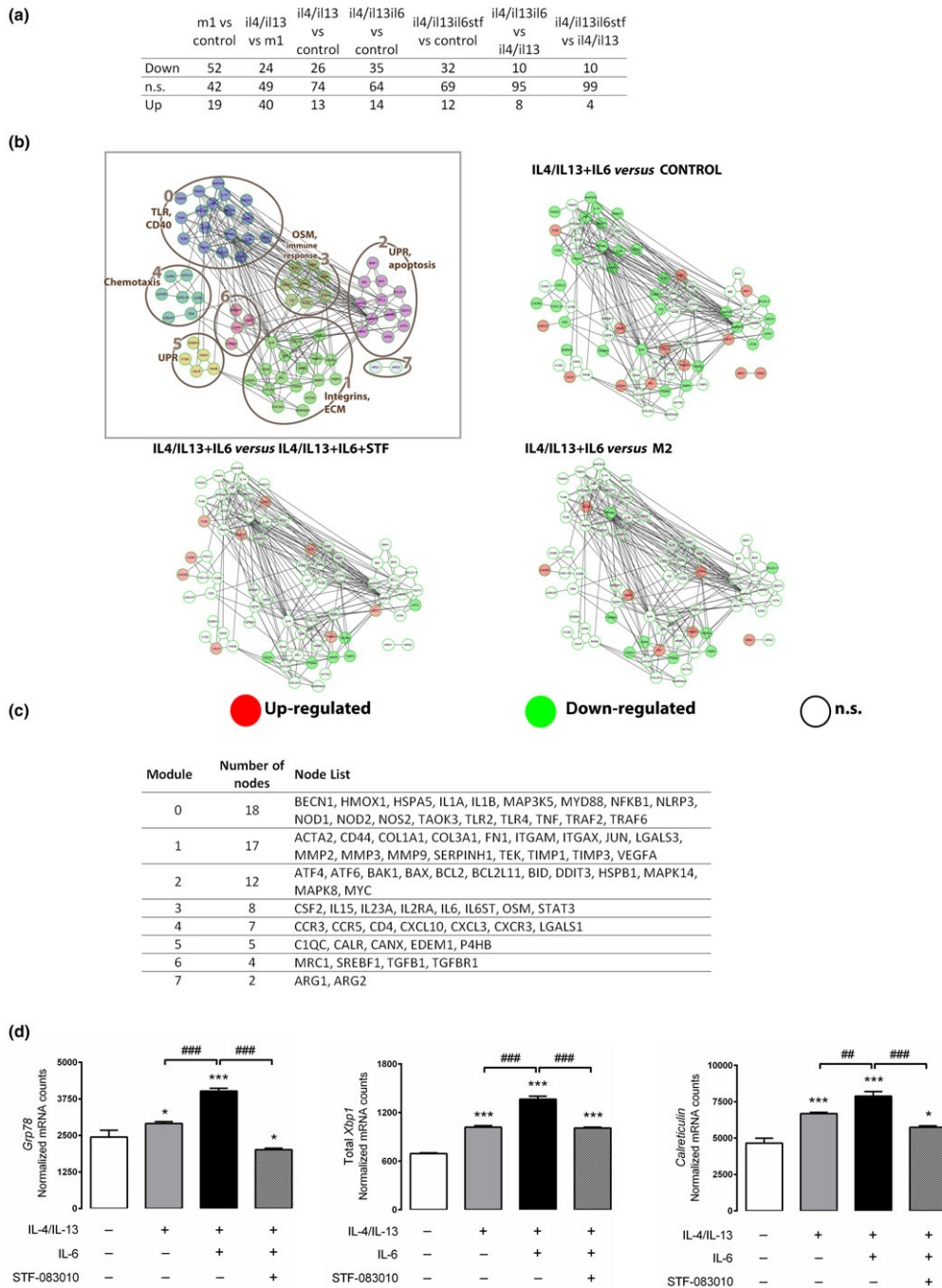


Figure 6. Significantly regulated gene numbers and functional networks with different modules and comparisons of interest showing downregulation of certain profibrotic related genes in hyper M2 macrophage treated with STF-083010. BMDMs were treated for 30 h with IL-4/IL-13, IL-4/IL-13+IL-6 and IL-4/IL-13+IL-6+STF-083010 phenotype and subsequently subjected for RNA isolation and NanoString gene expression. (a) Comparison of regulated and unregulated genes between different pairwise comparisons of interests. (b) Functional network and its regulation and (c) Gene list within each module. The network is consistent across all comparisons, while the regulation is marked by colors: upregulated genes are shown in red, downregulated—in green, and genes that were not found to be differentially expressed in the comparison of interest are shown in white. Functional network with different modules shown in different colors and marked by ellipses. Each ellipse contains the module ID and functional annotation. (d) Selected significantly regulated profibrotic related genes. * indicates $P < 0.05$; ## indicates $P < 0.01$; ***, ### indicates $P < 0.001$; where * represents a difference between any sample relative to the control unexposed group; # represents a difference between the indicated groups. [To see the full details shown within this figure, please go to the online version at <https://onlinelibrary.wiley.com/doi/10.1111/imcb.12212>.]

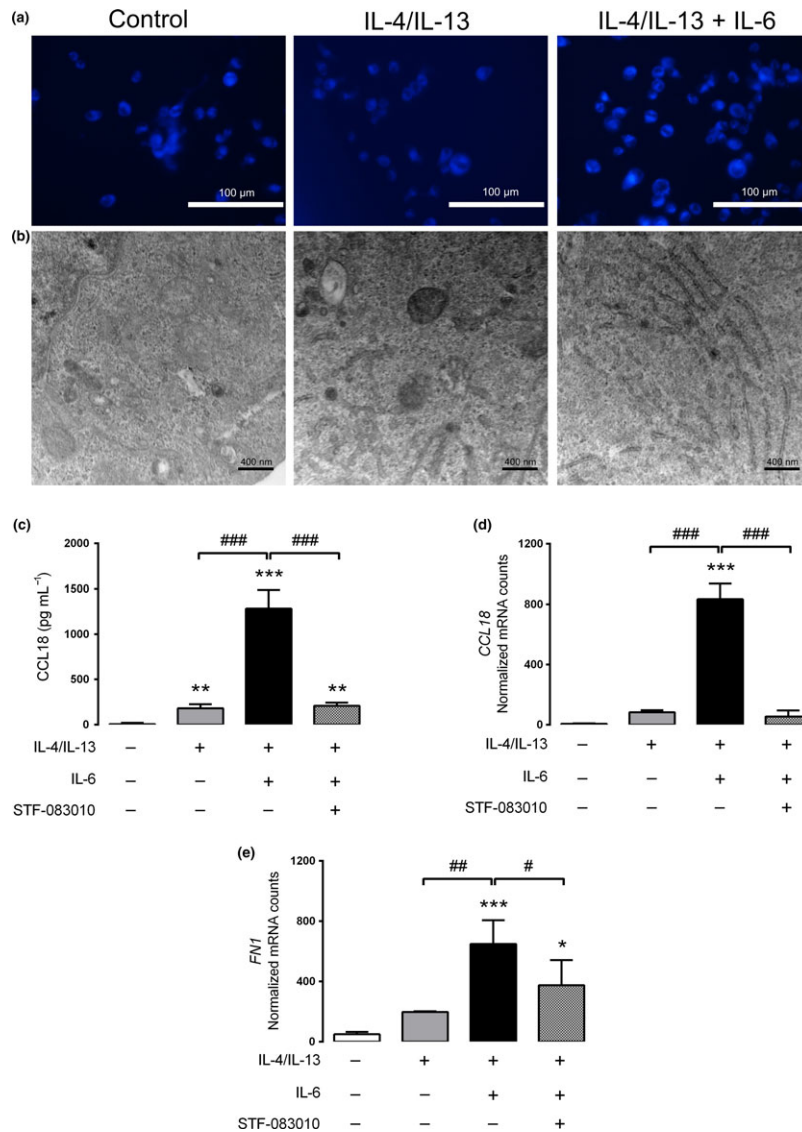


Figure 7. STF-083010 reduces ER size and the IL-6-mediated M2 phenotype of human macrophages. Human monocytic cell lines were differentiated into macrophages using PMA and then stimulated with IL-4/IL-13 and IL-4/IL-13+IL-6, alone or in combination with STF-083010 (for 72 h). **(a)** ER tracker (blue dye) and **(b)** transmission electron microscopy displaying the ER compartment. **(c, d)** In a separate experiment, CCL18 secretion and transcription was assessed as well as **(e)** the profibrotic related marker, *FN1*. Gene expression by NanoString is presented as normalized counts. A one-way ANOVA was used to assess the effect of each treatment. Data are presented as mean \pm s.e.m., each time point was assessed in quadruplicates. *, # indicates $P < 0.05$; **, ## indicates $P < 0.01$; ***, ### indicates $P < 0.001$; where * represents a difference between any sample relative to the control unexposed group; # represents a difference between the indicated groups.

macrophage polarization, the endoplasmic reticulum was quantitatively visualized and tracked using the ER tracker dye and transmission electron microscopy, respectively. In the living cells, ER distension was observed during IL-4/IL-13/IL-6-mediated polarization (Figure 7a). These findings were further supported by transmission electron microscopy, which showed enhanced ultrastructural changes of the ER (Figure 7b and Supplementary figure 9). Alternative activation was assessed by measuring the

secreted M2 marker, CCL18, in supernatants by ELISA as described earlier.²⁰ The addition of the IL-4/IL-13 polarizing cocktail resulted in a significant increase in CCL18 (from 5 ± 0.5 to 181.6 ± 15.6 pg mL⁻¹), consistent with previously published data,²¹ while the addition of IL-6 resulted in a sevenfold further increase in CCL18 (1283.0 ± 72.6 pg mL⁻¹) (Figure 7c). The addition of STF-083010 at 6 μ M normalized the effect of IL-6 and reduced the amount of CCL18 released to levels

comparable to IL-4/IL-13-mediated polarization cocktail ($208.3 \pm 12.6 \text{ pg mL}^{-1}$). Gene expression analysis indicated that *CCL18* mRNA expression was increased in a similar manner, mimicking the protein observations by IL-4/IL-13 exposure and highly upregulated by the addition of IL-6 (Figure 7d). Additionally, *FNI* was quantitated to reflect the profibrotic macrophage phenotype (please see Supplementary table 2 for information about the genes investigated). Consistent with our findings in murine-derived alternatively activated macrophages, STF-083010 also reduced the levels of secreted *CCL18* as well as *FNI* expression, reflecting its ability to prevent the “hyper” polarization mediated by IL-6 (Figure 7c–e). Overall, these findings are consistent with a critical role of an IL-6-mediated ER expansion program in macrophages that are alternatively activated both in murine and human systems.

DISCUSSION

Profibrotic, alternatively activated “M2” macrophages have been implicated in the pathogenesis of many different fibrotic diseases and cancers.²² Their interaction with fibroblasts and the fibrotic process has only been recently documented in literature.^{23–25} The “M2” phenotype can be induced by the binding of the pleiotropic cytokine IL-4 to its receptor, IL-4R α , which induces rapid tyrosine phosphorylation of STAT6, leading to the upregulation of the profibrotic M2-related phenotype.²⁶ Similar to *ex vivo* isolated macrophages, which are involved in pathological wound repair, IL-4/IL-13 stimulated macrophages may also share many of the factors involved in tissue repair. Therefore, to learn more about the behavior and phenotypic profibrotic functions of alternatively activated macrophages, it is important to understand: (1) the cellular organelles/mechanisms underlying macrophage polarization (IL-4/IL-13-mediated) and hyperpolarization (IL-4/IL-13/IL-6-mediated); (2) the profibrotic phenotype associated with these polarization states; and (3) whether the profibrotic phenotype of M2 macrophages can be attenuated.

It has been proposed that the IRE1-XBP1 axis is involved in the differentiation of many cell types that possess high secretory capacity through the activation of ER expansion programs.^{14,27} For instance, UPR-mediated XBP1 production and splicing has been implicated in B-cell to plasma cell differentiation,⁷ the differentiation of eosinophils⁵ as well as proper production of mucin from goblet cells.²⁸ Furthermore, IL-4 is one of the main Th2 cytokines that drives B cell differentiation into antibody-secreting plasma cells via an XBP1 dependent mechanism.²⁹ This led to the logical speculation that IL-4 and XBP1 might also be involved in ER membrane biogenesis and in the polarization of macrophages to the profibrotic M2 phenotype.

Interestingly, recent data have implicated IL-6 in augmenting the responses of macrophages to IL-4, and in subsequently enhancing the alternatively activated macrophage phenotype.¹ The inclusion of IL-6 with IL-4/IL-13 therefore provided a compelling model to study the hyper-polarization process of macrophages in relation to XBP1 induction and the profibrotic signature. Overall our data support the hypothesis that IL-6 can act synergistically with IL-4/IL-13 to augment spliced XBP1, leading to ER membrane expansion and the generation of a hyper profibrotic macrophage phenotype. With the use of bioinformatics analysis, we have been able to demonstrate the distinct transcriptional signatures induced by UPR-dependent macrophage polarization. These data provide evidence to the concept that IL-6 may act synergistically with IL-4 and IL-13 to increase the profibrotic capacity of alternatively activated macrophages. Additionally, our study suggests that targeting IRE1-endonuclease activity prevents the IL-6 dependent “hyper” profibrotic phenotype observed. Although STF-083010 was nontoxic to macrophages based on the cellular viability assay, we cannot fully exclude off-target effects of the drug. For example, the reduced phagocytic ability of the macrophage by STF-08010 can be one of these effects but it may establish a new link between XBP1 splicing, ER expansion and phagocytosis. However, more molecular and functional studies need to be designed to further dissect this phenomenon. In addition to the demonstrated role of the IRE1-XBP1 pathway, we also observed that ATF6 was highly induced in the IL-4/IL-13/IL-6 macrophage phenotype suggesting that the ATF6 pathway may be involved in regulating the expression of ER resident proteins, further enhancing ER membrane biogenesis. Consistent with this observation, Bommiasamy *et al.* reported that UPR-mediated ATF6 α activation could also promote ER expansion and phospholipid biosynthesis, independent of XBP1-splicing.³⁰ The mechanisms acted by ATF6 α could be distinct from those previously shown by XBP1, suggesting a redundant pathway executing a vital cellular task. While this process was investigated in stromal cells such as NIH-3T3 and CHO, it remains unclear whether it applies to the myeloid compartment—or whether activated ATF6 α is also involved to promote macrophage profibrotic activation. Further investigations revealed no significant alteration in the translational control arm of the UPR (p-PERK induction) even though there was a marked reduction in ATF4, a downstream marker of the PERK pathway.³¹ It has been recently reported that deleting ATF4 increases mitochondrial function and that ATF4 expression and mitochondrial function or density were inversely correlated in healthy tissues.³² Thus, it is tempting to speculate that the

enhanced mitochondrial mass could serve as a negative feedback loop to further downregulate their ATF4 expression, consistent with our observations when IL-6 is added to the M2 polarizing cocktail IL-4/IL-13. Furthermore, previous work done by Soto-Pantoja *et al.* showed that inhibition of IRE1 resulted in macrophages with increased mitochondrial oxygen consumption and extracellular acidification rate. This work may suggest that the increased mitochondrial mass seen in IL-4/IL-13/IL-6 macrophages may be a consequence of the increased mitochondrial demand needed because of XBP1 splicing induced by IL-6.³³ Although additional studies are required to assess how ATF4 and IRE1 influence mitochondrial and ER expansion and whether they are directly implicated in propagating the IL-4/IL-13/IL-6 macrophage, our findings collectively suggest that multiple UPR arms could devote a concerted effort into activating macrophage-ER expansion program, leading to enhanced profibrotic capacity.

The link between the relatively late timing of IRE1-XBP1 induction and the process of M2 polarization could suggest a late functional effect on macrophage profibrotic polarization. Our data demonstrate that the induction of spliced XBP1 correlated with the production of macrophage arginase activity during their polarization with IL-4/IL-13/IL-6. We did not find evidence for IL-6 alone to upregulate spliced XBP1 transcript counts, nor did we find evidence for IL-6 alone to modulate macrophage arginase activity, suggesting a true synergistic effect of IL-6 with IL-4/IL-13. Intriguingly, we observed that in the absence of M2 inducers, ER stress alone is insufficient to drive M2 macrophage polarity. This suggests that TH2 signals play more of a direct role in mediating the profibrotic as well as the ER and mitochondrial expansion phenotype observed in our studies. As IL-6 is increased during chronic tissue injury and some infections,³⁴ the finding that IL-6 may potentiate XBP1 induction in the presence of a Th2 milieu could have functional relevance to disease pathogenesis, and this remains to be precisely explored in future studies. Furthermore, given the observation that spliced XBP1 was not robustly increased during the first 10 h of polarization suggests that it may not be essential for initiation the M2-like phenotype but rather propagating the phenotype. It has been previously determined that IL-4/STAT6 axis is indispensable for the induction of alternative macrophage activation both *in vivo* and *in vitro*.³⁵ Thus, the precise mechanism by which XBP1 influences IL-4 dependent pathway activation and whether XBP1 selective inhibition is sufficient to ablate the macrophage profibrotic phenotype *in vivo* are valid approaches that remain under investigation.

Although IL-4/IL-13/IL-6-stimulated macrophages could represent a unique *in vitro* macrophage phenotype, *in vivo* macrophages are highly plastic and can continually alter their activation state and function depending on the cytokines and signals in their microenvironments.^{36,37} Using BMDMs and THP1-derived human macrophages, our data provide evidence that the IRE1-XBP1 pathway is modulated during ER expansion and profibrotic macrophage polarization. However, additional future experiments are needed to examine this pathway in tissue macrophages and monocyte-derived macrophages during disease pathogenesis and progression. Moreover, our data showed that the hyper profibrotic and molecular chaperone gene expression of IL-4/IL-13/IL-6-stimulated macrophages can be rescued with IRE1 inhibition. To further establish a functional profibrotic effect of the ER expansion pathway in these macrophages, future studies will need to take into consideration co-culture experiments with fibroblasts. Additionally, future work should be performed with IRE1-deficient macrophages, to identify a definitive mechanism between XBP1 and IL-6. Interestingly, it is thought that soluble mediators produced by M2 programmed macrophages enhance fibroblasts fibrogenicity by promoting their proliferation, collagen production and fibroblasts-to-myofibroblast differentiation.^{24,38} It is difficult to speculate if any or all of these processes are impacted by targeting ER expansion in macrophages. These experiments will yield novel and exciting data allowing for the better understanding of mechanisms underlying macrophage profibrotic activities. In addition, although it is acknowledged that ER stress may overwhelm the KDEL retrieval system and result in these proteins to migrate to the cell membrane and potentially limit the validity of KDEL assessment as an ER marker,³⁹ the data presented here were consistent with transmission electron microscopy quantifications of ER abundance.

In conclusion, the data presented suggests that the addition of IL-6 to the alternatively activated cocktail resulted in UPR activation as observed through ER expansion, and expression of profibrotic products. During this process, XBP1 splicing occurs to promote the expansion process and further enhance UPR activation to support the protein folding load within the ER. When IL-6 is present, it acts concurrently with IL-4 to synergize the above effects, thus further augmenting the UPR, ER expansion and profibrotic potential of the macrophage. Targeting ER expansion and IL-6 signaling in alternatively activated macrophages could be a valid strategy to lower the profibrotic cellular activity in diseases where M2-macrophages are known as primary cellular contributors.

METHODS

Isolation and polarization of bone marrow-derived macrophages

Bone marrow-derived macrophages were isolated and cultured as described previously (25). Briefly, bone marrow cells from C57BL/6 mice were isolated and treated with 20 ng mL⁻¹ M-CSF for 7 days. Following 7 days in culture, macrophages were exposed to recombinant murine IL-4 (20 ng mL⁻¹), IL-13 (50 ng mL⁻¹) and where applicable, IL-6 (5 ng mL⁻¹), for 24–120 h to induce alternative programming. Polarization to the M2-like phenotypes was assessed by arginase activity in cell lysates and by Arg1 and CD206 protein expression by flow cytometry. STF-083010 drug (Axon Medchem LLC, Reston, VA, USA) was solubilized in DMSO and used at 6 and 60 μM.

Arginase activity assay

The arginase activity assay on BMDMs was performed in-house, as shown previously.²

Western blotting

Western blotting of arginase-1 protein was performed as described previously.³

Phagocytosis assay

BMDMs were plated onto a 96-well tissue culture microplate (black with clear bottom plates, Falcon cat# 353219; Corning, New York, NY, USA) at a concentration of 100 000 cells per well. After 2 h, cells were induced with IL-4/IL-13, IL-4/IL-13/IL-6 and IL-4/IL-13/IL-6 plus STF-083010 (60 μM). After 30 h, the cytokines were washed off the cells and 1 μL of fluorescently tagged nanoparticles (Polysciences, Inc, Warrington, PA, USA; Cat# 17151) in 100 μL of media were added to each well and placed in an incubator for 3 h. Of note, wells of the same condition but with no beads served as internal controls. After 3 h, excess nanoparticles were washed off with warm PBS and fresh media was placed in each well. Uptake of the nanoparticles was determined by analyzing the plate in i3 SpectraMax plate reader (molecular devices). The nanoparticles were excited at 441 nm and the excitation photons were captured at a wavelength of 485 nm. Data were presented as ratio of nanoparticle treated well: no nanoparticle well, and denoted as Fluorescence (phagocytosis) index.

Immunofluorescence staining and quantification

BMDMs were isolated and cultured as previously described. Cells were lifted and plated on glass cover slips for polarization and treatment. Cells were fixed with 4% paraformaldehyde and

permeabilized using 0.1% Triton X. Immunofluorescence was completed for KDEL and TOMM20 to examine ER expansion and mitochondrial content, respectively. A FITC-labeled monoclonal mouse antibody was used against KDEL Dylight 488 conjugate (1:100) (Enzo Life Sciences, Burlington, ON, Canada; Cat# ADI-SPA-827-488-D). Following this, an antibody against TOMM20 (1:250) (Abcam, Toronto, ON, Canada; Cat# ab78547) was used with a donkey anti-rabbit secondary antibody (1:1000) (Abcam, Cat# ab150075). Immunofluorescence was performed to investigate the activation of the UPR. Cells were incubated with appropriate primary antibodies including anti-ATF4 (1:100) (Proteintech, Rosemont, IL, USA; Cat # 10835-1-AP), rabbit anti-pPERK (1:100) (Cell Signaling Technology, Danvers, MA, USA; Cat # 3179) with a donkey anti-rabbit-AF647 secondary antibody (1:1000) (Abcam, Cat # ab150075). Staining for ATF6 was also completed using a mouse anti-ATF6 primary antibody (1:100) (Novus Biologicals, Littleton, CO, USA; Cat # 70B1413.1) and a goat anti-mouse-AF647 secondary antibody (1:1000) (Thermo Fisher Scientific, Burlington, ON, Canada; Cat # A-21240). Images were taken at 40× magnification. ImageJ software (National Institutes of Health, Bethesda, MD, USA) was used to analyze and quantify antibody expression. All parameters were kept constant during imaging. Number of cells were counted and thresholding was used to detect percent positive area per cell. KDEL was analyzed at a threshold level of 80, TOMM20 was analyzed at 45 with DAPI at 32. ATF4, ATF6 and p-PERK were analyzed at a threshold level of 60, 50 and 50, respectively, while DAPI was set to 50, 35 and 35, respectively. DAPI was used to identify the nucleus of the cell which was used to identify the percent positive area of staining. This was completed using a blinded approach. Percent area of staining per cell was averaged for each experimental group.

Flow cytometry

Following polarization of BMDMs, ~1–2 × 10⁶ cells were subjected to FACS surface and intracellular staining protocol. Briefly, cells were initially suspended in FACS buffer solution (0.3% BSA in PBS; McMaster University, Hamilton, ON, Canada). Non-antigen-specific binding of immunoglobulins to Fcγ II/III receptor on BMDMs was blocked using purified rat anti-mouse CD16 (Mouse FC Block) (BD Pharmingen, Mississauga, ON, Canada; Cat#553142). Next, cells were subjected to surface antibody staining solution, containing a mix of anti-mouse F4/80 and anti-mouse CD206 (MMR) (BioLegend, San Diego, CA, USA; Cat#123133 and 141723). Cells were then fixed and permeabilized using BD Cytofix/Cytoperm solution (BD Biosciences, Mississauga, ON, Canada; Cat#554722) prior to performing intracellular staining with anti-mouse/human arginase-1 (1:5) (R&D Systems, Toronto, ON, Canada; Cat#IC5868A). Intracellular staining antibody solution was made up in 1× BD Perm/Wash buffer solution (BD Biosciences, Cat#554723). Cells were finally resuspended in FACS buffer for FACS and data were collected using BD LSRFortessa and FACSDiva software from BD Biosciences. Data were analyzed using FlowJo Software from Treestar.

Generation and treatment of THP-1-derived macrophages

The THP-1 human monocytic cell line was purchased from the American Type Culture Collection (ATCC#TIB-202). These suspended cells were grown in RPMI-1640 medium supplemented with 2 mM L-glutamine, 1% penicillin streptomycin and 10% FBS. THP-1 monocytes were differentiated into macrophages using phorbol myristate acetate (ATCC- 202152) at 10 ng mL⁻¹ for 48 h.⁴⁰ Macrophages were skewed toward the M2 phenotype using recombinant human IL-4 and IL-13 (20 and 20 ng mL⁻¹, respectively) and where applicable, recombinant human IL-6 (20 ng mL⁻¹; Peprotech, Montreal, QC, Canada) and STF-083010 (6 μM) were added. Exposure to the above cocktails lasted for 72 h before collection of supernatant and RNA isolation.

Transmission electron microscopy

BMDMs and THP-1-derived macrophages were seeded onto a six-well plate and polarized toward the macrophage phenotypes using the cytokine concentrations mentioned previously. Following their polarization, supernatant was collected and cells were washed twice with ice-cold PBS. Cells were then fixed in 2% glutaraldehyde in sodium cacodylate for 24 h. Cells were then post-fixed in osmium tetroxide, dehydrated in alcohol, lifted off the plate by propylene oxide, spun down into pellets and further processed for pellet embedding in epoxy resin. After polymerization, sections were stained with uranyl acetate and lead citrate and observed under a transmission electron microscope (Jeol TEMSCAN, Tokyo, Japan) by trained personnel in the Faculty of Health Sciences Electron Microscopy Core Facility at McMaster University. Image analysis was completed using ImageJ. ER was visualized as stacked cisternae membrane. The diameter of the cell was calculated using ImageJ, and the average distance from the nuclear membrane to the most distal portion of the ER was calculated. Percentage of ER was measured per macrophage, which was presented as the mean ± s.e.m., from five or more cells.

ER tracker assay

Following stimulation of THP1-derived macrophages, cells were washed twice with room temperature PBS and incubated with ER-Tracker Blue-White DPX at 1 μM (Thermo Fisher Scientific, Cat#E123533) for 30 min at room temperature. The cells were washed twice with cold PBS and images were taken with the EVOS FL Cell Imaging System.

ELISA

Human CCL18/PARC protein was assessed in the cell culture supernatant using the commercially available CCL18 ELISA, according to the manufacturer's protocol (R&D Systems, Cat# DCL180B).

RNA extraction and assessment of RNA quality

Total RNA from BMDMs and THP-1-derived macrophages was isolated using Nucleospin RNA plus [D-Mark BioSciences, Toronto, Canada (Catalog No. MN-740984.250)]. Concentrations and RNA purity were measured using a NanoVue spectrophotometer (V1.7.3). The integrity and quantity of the RNA were examined using the Agilent Bioanalyzer 2100 (Agilent Technologies, Santa Clara, CA, USA) before NanoString gene expression analysis.

Real-time polymerase chain reaction

mRNA isolated from BMDMs reverse-transcribed using Superscript II RT (Invitrogen, Carlsbad, California, USA) to obtain cDNA for gene expression analysis. A 7500 Real-Time PCR Machine (Applied Biosystems, Foster City, CA, USA) with fast SYBR green mix (Applied Biosystems, Foster City, CA, USA, Catalog No. 4385612) were employed. The PCR protocol used was a 20-s initiation at 50°C, followed by 10 min at 95°C, 40 cycles of 15 s amplification at 95°C and 1 min at 60°C. SYBR green primers, including *spliced Xbp1*, forward, 5'-TCCGCAGCAGGTGCAGG-3', and reverse, 5'-GCCCAAAGGATATCAGACTCAGA-3' and for *18S*, forward, 5'-AGTCCTGCCCTTTGTACACA-3', and reverse, 5'-CGATCCGAGGGCCTCACT-3' were produced by the DNA Sequencing and Oligo Synthesis Facility at McMaster University (MOBIX Lab). *18s* was used as reference gene to assess *spliced X-box binding protein 1* mRNA gene expression. Candidate genes were analyzed using semi-quantitative gene expression analysis (ΔΔCT method) and expressed as fold change relative to the gene expression of the control untreated BMDMs.

Nanostring analysis

Nanostring gene expression profiling was performed on murine BMDM as well as THP-1-derived macrophages (only selected genes for THP-1 cells). We performed multiplexed target profiling of inflammation- and immune-related transcripts on Control, IL-4/IL-13, IL-4/IL-13+IL-6 and IL-4/IL-13+IL-6+STF-083010 samples. Pre-processing and normalization was performed with nSolver 2.5 software (www.nanostring.com) using six negative controls for background subtraction and six positive controls for normalization. Next total counts normalization was performed. All genes were used to perform PCA and visualize the first 3 components (Bioconductor, rgl package; <https://cran.r-project.org/web/packages/rgl/index.html>, The R Foundation for Statistical Computing, Vienna, Austria), and to perform hierarchical clustering (using euclidean distance and average linkage). The "limma" package and differential expression in microarray experiments were performed as described previously.

Network analysis of nanostring data

Networks were constructed using Cytoscape software.⁴¹ Reactome FI plugin was used to build functional networks, which were then analyzed for the presence of significant modules (gene clusters).⁴²

These modules were further examined with Pathway enrichment and Gene Ontology (GO) tools in Cytoscape. Functional networks contain the differentially regulated genes within the indicated biological process and do not necessarily include all other significantly regulated genes.

Statistical analysis

Results are expressed as mean \pm s.e.m. A one-way analysis of variance (one-way ANOVA) followed by Tukey's post hoc tests were used to determine significance when more than two groups were compared. A Student's *t*-test was used to determine significance between two conditions. All statistical tests were performed using GraphPad Prism 7.0c (GraphPad Software, La Jolla, CA, USA). A $P < 0.05$ was considered statistically significant.

Data availability

The datasets generated during and/or analyzed during the current study are available from the corresponding author on reasonable request.

ACKNOWLEDGMENTS

We sincerely thank the electron microscope facility (McMaster University, ON, Canada) for their exceptional training and technical service. We thank Christine King and Liliana De Sousa (Farncombe Metagenomics Facility, McMaster University, ON, Canada) for help with NanoString experiments. This work was performed with funding from the Ontario Thoracic Society (Canadian Lung Association). This work was funded partly by the Canadian Institute of Health Research (CIHR; Grant No. 137013) and the Ontario Thoracic Society (Canadian Lung Association) awarded to KA and CDR. EAA is funded by the Canadian Institute of Health Research (CIHR; Grant No. 140358). AA is funded by Ontario Graduate Scholarships (OGS) and by Eva Eugenia Lillian Cope Graduate scholarship.

CONFLICT OF INTEREST

All authors declare no competing financial interests.

REFERENCES

- Mauer J, Chaurasia B, Goldau J, et al. Signaling by IL-6 promotes alternative activation of macrophages to limit endotoxemia and obesity-associated resistance to insulin. *Nat Immunol* 2014; **15**: 423–430.
- Ayaub EA, Dubey A, Imani J, et al. Overexpression of OSM and IL-6 impacts the polarization of pro-fibrotic macrophages and the development of bleomycin-induced lung fibrosis. *Sci Rep* 2017; **7**: 13281.
- Dubey A, Izakelien L, Ayaub EA, et al. Separate roles of IL-6 and oncostatin M in mouse macrophage polarization *in vitro* and *in vivo*. *Immunol Cell Biol* 2018; **96**: 257–272.
- Dickhout JG, Lhotak S, Hilditch BA, et al. Induction of the unfolded protein response after monocyte to macrophage differentiation augments cell survival in early atherosclerotic lesions. *Faseb J* 2010; **25**: 576–589.
- Bettigole SE, Lis R, Adoro S, et al. The transcription factor XBP1 is selectively required for eosinophil differentiation. *Nat Immunol* 2015; **16**: 829–837.
- Iwakoshi NN, Pypaert M, Glimcher LH. The transcription factor XBP-1 is essential for the development and survival of dendritic cells. *J Exp Med* 2007; **204**: 2267–2275.
- Reimold AM, Iwakoshi NN, Manis J, et al. Plasma cell differentiation requires the transcription factor XBP-1. *Nature* 2001; **412**: 300–307.
- Grootjans J, Kaser A, Kaufman RJ, et al. The unfolded protein response in immunity and inflammation. *Nat Rev Immunol* 2016; **16**: 469–484.
- Wu R, Zhang QH, Lu YJ, et al. Involvement of the IRE1alpha-XBP1 pathway and XBP1s-dependent transcriptional reprogramming in metabolic diseases. *DNA Cell Biol* 2015; **34**: 6–18.
- Martinon F, Chen X, Lee AH, et al. TLR activation of the transcription factor XBP1 regulates innate immune responses in macrophages. *Nat Immunol* 2010; **11**: 411–418.
- Roszer T. Understanding the mysterious M2 macrophage through activation markers and effector mechanisms. *Mediators Inflamm* 2015; **2015**: 816460.
- Gensel JC, Kopper TJ, Zhang B, et al. Predictive screening of M1 and M2 macrophages reveals the immunomodulatory effectiveness of post spinal cord injury azithromycin treatment. *Sci Rep* 2017; **7**: 40144.
- Bettigole SE, Glimcher LH. Novel roles for XBP1 in hematopoietic development. *Cell Cycle* 2016; **15**: 1653–1654.
- Shaffer AL, Shapiro-Shelef M, Iwakoshi NN, et al. XBP1, downstream of Blimp-1, expands the secretory apparatus and other organelles, and increases protein synthesis in plasma cell differentiation. *Immunity* 2004; **21**: 81–93.
- Upagupta C, Carlisle RE, Dickhout JG. Analysis of the potency of various low molecular weight chemical chaperones to prevent protein aggregation. *Biochem Biophys Res Commun* 2017; **486**: 163–170.
- Zhao X, Yang H, Liu W, et al. Sec22 regulates endoplasmic reticulum morphology but not autophagy and is required for eye development in *Drosophila*. *J Biol Chem* 2015; **290**: 7943–7951.
- Burbulla LF, Fitzgerald JC, Stegen K, et al. Mitochondrial proteolytic stress induced by loss of mortalin function is rescued by Parkin and PINK1. *Cell Death Dis* 2014; **5**: e1180.
- Contino S, Porporato PE, Bird M, et al. Presenilin 2-dependent maintenance of mitochondrial oxidative capacity and morphology. *Front Physiol* 2017; **8**: 796.
- Kawalec M, Boratynska-Jasinska A, Beresewicz M, et al. Mitofusin 2 deficiency affects energy metabolism and mitochondrial biogenesis in MEF cells. *PLoS ONE* 2015; **10**: e0134162.

20. Schutyser E, Richmond A, Van Damme J. Involvement of CC chemokine ligand 18 (CCL18) in normal and pathological processes. *J Leukoc Biol* 2005; **78**: 14–26.
21. Schupp JC, Binder H, Jager B, *et al.* Macrophage activation in acute exacerbation of idiopathic pulmonary fibrosis. *PLoS ONE* 2015; **10**: e0116775.
22. Wynn TA, Vannella KM. Macrophages in tissue repair, regeneration, and fibrosis. *Immunity* 2016; **44**: 450–462.
23. Van Linthout S, Miteva K, Tschope C. Crosstalk between fibroblasts and inflammatory cells. *Cardiovasc Res* 2014; **102**: 258–269.
24. Ploeger DT, Hospers NA, Schipper M, *et al.* Cell plasticity in wound healing: paracrine factors of M1/M2 polarized macrophages influence the phenotypical state of dermal fibroblasts. *Cell Commun Signal* 2013; **11**: 29.
25. Liu XQ, Kiefl R, Roskopf C, *et al.* Interactions among lung cancer cells, fibroblasts, and macrophages in 3D Co-cultures and the impact on MMP-1 and VEGF expression. *PLoS ONE* 2016; **11**: e0156268.
26. Wang N, Liang H, Zen K. Molecular mechanisms that influence the macrophage m1-m2 polarization balance. *Front Immunol* 2014; **5**: 614.
27. Niederreiter L, Fritz TM, Adolph TE, *et al.* ER stress transcription factor Xbp1 suppresses intestinal tumorigenesis and directs intestinal stem cells. *J Exp Med* 2013; **210**: 2041–2056.
28. Tsuru A, Fujimoto N, Takahashi S, *et al.* Negative feedback by IRE1beta optimizes mucin production in goblet cells. *Proc Natl Acad Sci USA* 2013; **110**: 2864–2869.
29. Iwakoshi NN, Lee AH, Vallabhajosyula P, *et al.* Plasma cell differentiation and the unfolded protein response intersect at the transcription factor XBP-1. *Nat Immunol* 2003; **4**: 321–329.
30. Bommasamy H, Back SH, Fagone P, *et al.* ATF6alpha induces XBP1-independent expansion of the endoplasmic reticulum. *J Cell Sci* 2009; **122**: 1626–1636.
31. Rozpedek W, Pytel D, Mucha B, *et al.* The role of the PERK/eIF2alpha/ATF4/CHOP signaling pathway in tumor progression during endoplasmic reticulum stress. *Curr Mol Med* 2016; **16**: 533–544.
32. Quiros PM, Prado MA, Zamboni N, *et al.* Multi-omics analysis identifies ATF4 as a key regulator of the mitochondrial stress response in mammals. *J Cell Biol* 2017; **216**: 2027–2045.
33. Soto-Pantoja DR, Wilson AS, Clear KY, *et al.* Unfolded protein response signaling impacts macrophage polarity to modulate breast cancer cell clearance and melanoma immune checkpoint therapy responsiveness. *Oncotarget* 2017; **8**: 80545–80559.
34. Tanaka T, Narazaki M, Kishimoto T. IL-6 in inflammation, immunity, and disease. *Cold Spring Harb Perspect Biol* 2014; **6**: a016295.
35. Ohmori Y, Hamilton TA. STAT6 is required for the anti-inflammatory activity of interleukin-4 in mouse peritoneal macrophages. *J Biol Chem* 1998; **273**: 29202–29209.
36. Sica A, Mantovani A. Macrophage plasticity and polarization: *in vivo* veritas. *J Clin Invest* 2012; **122**: 787–795.
37. Das A, Sinha M, Datta S, *et al.* Monocyte and macrophage plasticity in tissue repair and regeneration. *Am J Pathol* 2015; **185**: 2596–2606.
38. Zhu Z, Ding J, Ma Z, *et al.* Alternatively activated macrophages derived from THP-1 cells promote the fibrogenic activities of human dermal fibroblasts. *Wound Repair Regen* 2017; **25**: 377–388.
39. Zhang Y, Liu R, Ni M, *et al.* Cell surface relocalization of the endoplasmic reticulum chaperone and unfolded protein response regulator GRP78/BiP. *J Biol Chem* 2010; **285**: 15065–15075.
40. Park EK, Jung HS, Yang HI, *et al.* Optimized THP-1 differentiation is required for the detection of responses to weak stimuli. *Inflamm Res* 2007; **56**: 45–50.
41. Shannon P, Markiel A, Ozier O, *et al.* Cytoscape: a software environment for integrated models of biomolecular interaction networks. *Genome Res* 2003; **13**: 2498–2504.
42. Wu G, Stein L. A network module-based method for identifying cancer prognostic signatures. *Genome Biol* 2012; **13**: R112.

SUPPORTING INFORMATION

Additional supporting information may be found online in the Supporting Information section at the end of the article.

© 2018 The Authors
Immunology & Cell Biology published by John Wiley & Sons Australia, Ltd on behalf of Australasian Society for Immunology Inc.

This is an open access article under the terms of the Creative Commons Attribution-NonCommercial License, which permits use, distribution and reproduction in any medium, provided the original work is properly cited and is not used for commercial purposes.